Catal Lett (2009) 128:423–433
DOI 10.1007/s10562-008-9768-y

Influence of the Reaction Temperature on the 3-Hexyne Semi-Hydrogenation Catalyzed by a Palladium(II) Complex

D. A. Liprandi · E. A. Cagnola · M. E. Quiroga · P. C. L'Argentière

Received: 27 August 2008 / Accepted: 5 October 2008 / Published online: 23 December 2008

Abstract The dichlorobis (tridecylamine) palladium(II) complex, pure and supported on γ-Al_2O_3, was used as catalyst for the semi-hydrogenation of 3-hexyne. The complex was characterized by centesimal composition, XPS and IR. The influence of the temperature was studied. The supported Pd complex resulted an active and stereo selective system for the production of (*Z*)-3-hexene.

Keywords Palladium complex · Alkynes semi-hydrogenation · (*Z*)-3-hexene production · Lindlar catalyst

1 Introduction

The major utility of selective alkyne hydrogenation has been established for the synthesis and manufacture of fine and industrial chemicals (e.g., food additives, flavors and fragrances, pharmaceutical, agrochemicals, and petrochemical industries) [1]. Regarding non-terminal alkyne semi-hydrogenation, the main goal is to achieve the highest possible conversion and selectivity to the (*Z*)-alkene [2]. The most widely common catalysts that have been researched for five decades are based on palladium species, but selectivity rarely exceeds 90% [3]. Among them it can be mentioned the Lindlar catalyst (5 wt% palladium heterogenized on calcium carbonate poisoned by lead acetate or lead oxide, Pd–$CaCO_3$–Pb) [4].

Within the Group VIII transition metals (Pt, Pd, Rh, Ru, Ni), palladium is regarded as the most efficient catalyst for the semi-hydrogenation of mono-substituted acetylenes, and of terminal and internal alkynes [1–3, 5–8]. The pronounced selectivity of palladium is attributed to the fact that the chemisorption of the alkyne species on the active centre is stronger than that of the alkene. This, in turn, is related to the restricted rotation of the C–C triple bond and to the high electron density in an alkyne species [2].

Some authors studied the influence of different supports on the performance of Pd catalysts used for this kind of hydrogenation of alkynes. Choudary et al. [5] concluded that some Pd-exchanged mesoporous materials, such as Pd/Si-K10 and Pd/MCM-41, gave satisfactory results for the semi-hydrogenation of non terminal alkynes. Gruttadauria et al. [9] employed pumice as support; these authors stated that the good activity and selectivity to the obtained alkene were probably due to the presence of sodium ions in the pumice structure that increases the electron density on the supported metal. Lennon et al. [10] studied the rate of hydrogenation of a terminal alkyne (propyne) under continuous flow conditions using Pd/C as catalyst; the authors concluded that the rate of hydrogenation is critically dependent on the concentration of hydrogen. Marin-Astorga et al. [11] reported high selectivities to (*Z*)-alkene obtained for the

D. A. Liprandi (✉) · E. A. Cagnola · M. E. Quiroga · P. C. L'Argentière
Química Inorgánica, Departamento de Química, Facultad de Ingeniería Química, Universidad Nacional Del Litoral (UNL), 3000 Santiago del Estero, Santa Fe 2829, Argentina
e-mail: dlipran@fiqus.unl.edu.ar

E. A. Cagnola
e-mail: ecagnola@fiqus.unl.edu.ar

M. E. Quiroga · P. C. L'Argentière
INCAPE, Instituto de Investigaciones en Catálisis y Petroquímica (FIQ-UNL, CONICET), 3000 Santiago del Estero, Santa Fe 2654, Argentina

M. E. Quiroga
e-mail: mquiroga@fiqus.unl.edu.ar

P. C. L'Argentière
plargent@fiqus.unl.edu.ar

hydrogenation of internal aromatic alkynes on palladium supported catalysts using different siliceous supports such amorphous SiO_2, mesoporous MCM-41 and silylated MCM-41. For similar reactions (1-phenyl-1-butyne, 1-phenyl-1-pentyne, phenyl-acetylene, 4-octyne), the hydrophobic Pd-montmorillonite has also proved to be highly efficient catalysts, their selectivities to (*Z*)- species (around 90%) being comparable with that of the Lindlar catalyst [6, 12]. Mastalir and Király [2] tested Pd nanoparticles on hydrotalcite, which proved to be efficient catalysts for liquid phase semi-hydrogenation on both terminal and internal alkynes.

To improve the selectivity to the partial reduction of triple bonds, some authors used quinoline and triphenylphosphine as additives in the heterogeneous semi-hydrogenation of alkynes. Yu and Spencer [13] demonstrated that quinoline and triphenylphosphine species act as ligands for heterogeneous palladium and alter the electronic properties of the metal thus increasing the selectivity. Nijhuis et al. [14] showed that the primary function of this type of modifiers is to decrease the reaction rate; in this way the lower catalyst activity results in the higher selectivity.

In the last decades few authors studied catalytic selectivity to (*Z*)- alkenes semi-hydrogenation of internal alkynes using other metal or bimetallic catalysts. Brown and Ahuja [15] found that P-2 nickel (an amorphous mixture of nickel and boron) is an excellent catalyst for selective partial hydrogenation of dialkylacetylenes to (*Z*)-olefins. Choi and Yoon [16] utilized nickel boride (supported on a borohydride exchange resin) as catalyst at low temperatures (273 K) to study the (*Z*)-selective semi-hydrogenation of acetylenes; the authors concluded that the selectivity could be enhanced by lowering the reaction temperature up to 258 K. Guczi et al. [17] proved that systems containing Cu partially alloyed with Pd are more active and selective towards the hydrogenation of phenylacetylene. Coq and Figueras [18] studied the influence of co-metals on the performance of Pd bimetallic catalysts used in the semi-hydrogenation of alkynes. Nijhuis et al. [19] modified palladium catalysts with copper, improving the selectivity for functionalized alkynes semi-hydrogenation.

Finally, transition metal complexes have been widely used as catalysts for homogeneous and heterogeneous hydrogenation reactions. It was reported that higher activities and selectivity's could be attained with these catalysts than with conventional ones. In addition, metal complex-based catalysts were shown to be active under mild conditions of temperature and pressure. Palladium, rhodium and ruthenium complexes were employed as efficient catalysts for terminal alkynes semi-hydrogenation [20–24]. However, few authors studied the performance of metal complexes, via homogeneous or heterogeneous processes, for the selective hydrogenation of high molecular weight non terminal alkynes [2, 22, 25].

In previous papers we have studied the catalytic activity and the selectivity of the $[PdCl_2(NH_2(CH_2)_{12}CH_3)_2]$ complex for the semi-hydrogenation of a relative high molecular weight terminal alkyne: 1-heptyne, under mild conditions of temperature and pressure in homogeneous and heterogeneous systems, using alumina and activated carbons as supports [26, 27]. Under the same operational conditions the heterogeneous catalysts, obtained supporting $[PdCl_2(NH_2(CH_2)_{12}CH_3)_2]$ on γ-Al_2O_3 or on a micro porous carbon, are more active and selective for the semi-hydrogenation of the terminal alkyne than the classic Lindlar's catalyst. As determined by X-ray photoelectron spectroscopy and Fourier transform infrared spectroscopy the active species is the complex itself, which is stable under the reaction conditions [26, 27]. Considering the semi-hydrogenation of 1-heptyne, the location of the active phase (the complex) in the porous network of the support could increase the selectivity to the planar double bond end of the 1-heptene molecules; certain size and shape of the pores can also enhance selectivity. In this sense, activated carbons have the advantage of slit-shaped pores [27] inducing shape selectivity.

The objective of this work is to study the influence of the reaction temperature on the semi-hydrogenation of 3-hexyne, a relative high molecular weight non terminal alkyne, using dichlorobis (tridecylamine) palladium(II) as catalyst in homogeneous and heterogeneous conditions. Activity and selectivity of the Pd(II) complex are evaluated and compared against those obtained with the conventional Lindlar catalyst.

2 Experimental

Anhydrous palladium(II) chloride (purity > 99%, Catalogue No. 2315962) and tridecylamine (purity > 99%, Catalogue No. 91590) were Fluka products. Toluene (purity > 99.5%, Catalogue No. TX0735-44) chloroform (purity 99–99.4%, Catalogue No. 1.02445) and methanol (purity > 99.8%, Catalogue No. 476.15827) were Merck products. Potassium bromide (purity > 90%, Catalogue No. 22,186-4, FTIR grade) and Cesium iodide (purity > 99%, Catalogue No. 28,935-3), 3-hexyne (purity > 99% Catalogue No. 30,689-4) and the Lindlar catalyst (palladium 5 wt% on calcium carbonate, poisoned with lead, Catalogue No. 20,573-7) were Aldrich products.

The complex synthesis and purification were fully described in a previous publication [28]. In summary, the complex was prepared by reaction of $PdCl_2$ with tridecylamine ($CH_3(CH_2)_{12}NH_2$, from now named TDA), with a molar ratio TDA/Pd = 2, using toluene as solvent at 358 K. The final purification of the metal complex was made by column chromatography, using silica gel as

stationary phase and chloroform as solvent. The obtained complex is soluble in organic solvents, such as chloroform, toluene and chloroform–methanol solutions.

The incipient wetness technique [29] was used to carry out the heterogenization of the Pd complex on γ-alumina Ketjen CK 300 (cylinders of 1.5 mm diameter). The support was previously calcined in air at 773 K for 3 h, obtaining a material with BET surface area: 180 $m^2\ g^{-1}$, and pore volume: 0.52 $cm^3\ g^{-1}$. A solution of the palladium complex in chloroform was used for impregnation in a suitable concentration to obtain a catalyst containing 0.3 wt% Pd. A mass of 0.075 g of alumina was used in each catalytic test. The procedure was carried out at 298 K and after that the complex/γ-Al_2O_3 system was put into a desiccator till constant mass was verified.

The reaction test was the 3-hexyne semi-hydrogenation. For comparative purposes, the following catalysts without any pre-treatment were evaluated: (1) $[PdCl_2(NH_2(CH_2)_{12}CH_3)_2]$ unsupported, (2) alumina supported $[PdCl_2(NH_2(CH_2)_{12}CH_3)_2]$ complex, (3) commercial Lindlar catalyst. In all the cases a 2% (v/v) solution of 3-hexyne in toluene was used, and with a 3-hexyne/Pd molar ratio equal to 8,400.

The reaction was carried out in a batch stainless-steel stirred tank reactor, $V = 100$ mL and stirring velocity 600 rpm, operated at 150 kPa of hydrogen pressure during 120 min. Both the reactor and the stirrer were poly (tetrafluoroethylene) coated in order to avoid the possible contamination of the reaction media with metal cations. The possibility of diffusional limitations present in the catalytic tests performed was investigated [30, 31]. Experiments were carried out at different stirring velocities in the range 180–1,400 rpm. The constancy of activity and selectivity above 500 rpm, ensured that external limitations were absent at the rotary speed selected. On the other hand, to ensure that the catalytic results were not influenced by intraparticle mass-transfer limitations, the heterogenized complex catalyst was crushed up to 1/4 of the original size of the γ-Al_2O_3 pellets used as support. Then, several runs using the crushed complex catalyst were carried out. In every case, the conversion and selectivity values obtained were the same than those corresponding to the catalyst that was not crushed. Hence it may be concluded that internal diffusional limitations were absent in the operational conditions of this work. Last but not least, the catalyst cylinders were properly treated and weighted after end of reaction. The difference in the mass of catalyst cylinders (before and after the test reaction) was within the experimental error of the analytical balance method, meaning that there was no mass loss from the cylinders. Thus, it can be considered that the attrition effect is absent or is negligible enough to play a role in determining an additional mass transfer limitation.

To study the influence of the reaction temperature on each catalytic test, a set of runs were performed, at $T_1 = 275$ K, $T_2 = 290$ K, and $T_3 = 303$ K. Reactants and products were analyzed by gas chromatography, using a flame ionization detector and a CP WAX 52 CB capillary column. All runs were carried out in triplicate; the relative experimental error was about 3%.

The presence and weight percent of palladium, chlorine and nitrogen elements were evaluated by analytical chemical techniques for the pure complex on a C- and H- free base, as reported elsewhere [32].

Following a procedure previously described [28], the electronic state of Pd in the Lindlar catalyst, and of Pd, N and Cl and their atomic ratios in the alumina supported and unsupported complex were studied by XPS. Determinations were carried out on a Shimadzu ESCA 750 electron spectrometer coupled to a Shimadzu ESCAPAC 760 Data System. The superficial electronic states of palladium, nitrogen and chlorine were studied following the position of the maximum of the Pd $3d_{5/2}$, N $1s_{1/2}$ and Cl $2p_{3/2}$ peaks, respectively; the C $1s_{1/2}$ line was taken as an internal standard at 285.0 eV, as previously described [33].

The infrared wave numbers corresponding to TDA, $[PdCl_2(TDA)_2]$ and the alumina supported $[PdCl_2(TDA)_2]$ fresh and after the reaction tests, were analyzed in the 4,600–200 cm^{-1} range in a Shimadzu FTIR 8101/8101 M single beam spectrometer (equipment I) following a procedure previously reported [32]. Due to the low detector sensitivity below 500 cm^{-1}, a Perkin-Elmer 580 B double beam spectrometer (equipment II) was also used. The characteristic group wave numbers corresponding to the $CH_3(CH_2)_{12}NH_2$ molecule were used to determine whether the palladium complex kept its identity after heterogenization and after being used in the test reaction. All the samples were dried at 353 K and were examined either in potassium bromide or cesium iodide disks in a concentration ranging from 0.5 to 1 wt% to ensure non-saturated spectra [34].

The possibility of complex leaching from the supported catalyst during the hydrogenation tests was verified by means of the following procedures: (1) XPS determinations of the Pd/Al atomic ratios for the catalyst after each catalytic test; (2) spectrophotometric determinations to analyze Pd in the remaining solutions after each catalytic run; (3) spectrophotometric determinations to analyze Pd in the remaining solution after carrying out a blank test performed with the supported complex in pure toluene for 100 h under the operational conditions of this work.

3 Results

The elemental composition (wt%) for Pd, N and Cl obtained for the pure complex on a C- and H- free base were 52.0, 13.7, and 34.3, respectively, being the Cl/Pd and N/Pd molar ratios 1.99 and 2.00, respectively.

Table 1 XPS results for the unsupported and fresh supported palladium complex

Sample	Pd $3d_{5/2}$ (eV)	N $1s_{1/2}$ (eV)	Cl $2p_{3/2}$ (eV)	Pd/Al (at/at)	N/Pd (at/at)	Cl/Pd (at/at)
[Pd-TDA]	338.2	401.9	198.3	–	2.00	1.99
[Pd-TDA]/γ-Al_2O_3	338.3	401.7	198.2	0.088	2.01	2.00

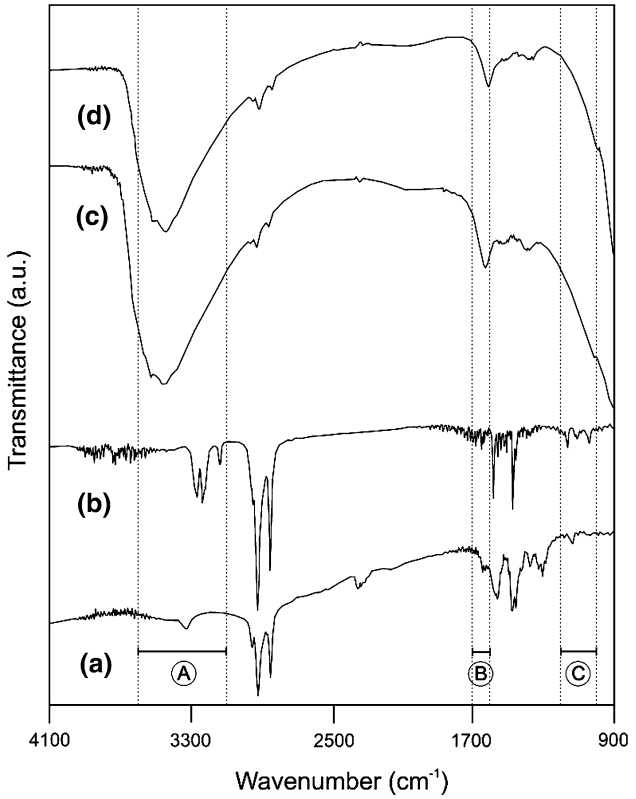

Fig. 1 FTIR spectra obtained for: *a* pure TDA, *b* pure $[PdCl_2(NH_2(CH_2)_{12}CH_3)_2]$, *c* fresh alumina supported $[PdCl_2(NH_2(CH_2)_{12}CH_3)_2]$, *d* alumina supported $[PdCl_2(NH_2(CH_2)_{12}CH_3)_2]$ after hydrogenation evaluations at 303 K and 150 kPa. Zones (A) NH_2 stretching (3,400–3,100 cm^{-1}); (B) NH_2 bending (1,700–1,600 cm^{-1}); and (C) CN stretching (1,200–1,000 cm^{-1})

Table 1 shows the Pd $3d_{5/2}$, Cl $2p_{3/2}$ and N $1s_{1/2}$ peaks binding energies (BE), and the atomic ratios Cl/Pd and N/Pd for the unsupported complex and for the fresh supported complex. In Table 1 is also displayed the superficial atomic ratio of Pd/Al for the alumina supported palladium complex. The Pd $3d_{5/2}$ peak BE for the Lindlar catalyst was 337.2 eV.

The following samples were analyzed by FTIR spectroscopy in the 4,600–200 cm^{-1} range (equipment I): (1) pure TDA, (2) pure $[PdCl_2(NH_2(CH_2)_{12}CH_3)_2]$, (3) fresh alumina supported $[PdCl_2(NH_2(CH_2)_{12}CH_3)_2]$, (4) alumina supported $[PdCl_2(NH_2(CH_2)_{12}CH_3)_2]$ after 3-hexyne hydrogenation at 303 K. The spectra are shown in Fig. 1. Pure palladium complex unsupported and supported on γ-Al_2O_3 were also analyzed in the range 800–200 cm^{-1} using equipment II; the spectra are presented in Fig. 2.

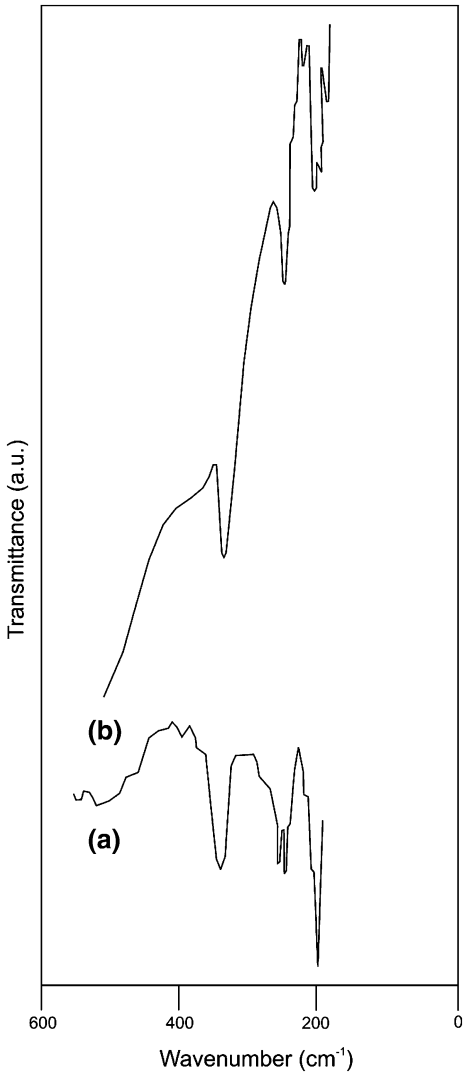

Fig. 2 IR spectra below 500 cm^{-1} of samples: *a* pure $[PdCl_2(NH_2(CH_2)_{12}CH_3)_2]$, *b* fresh alumina supported $[PdCl_2(NH_2(CH_2)_{12}CH_3)_2]$

During the catalytic tests the only products detected were: (*Z*)-3-hexene, (*E*)-3-hexene and *n*-hexane. The results obtained for the semi-hydrogenation of the internal aliphatic alkyne, 3-hexyne, over the Lindlar, the supported or unsupported $[PdCl_2(TDA)_2]$ catalysts, are depicted in Figs. 3, 4, 5, 6, 7, 8. In these figures the conversions to (*Z*)-3-hexene ($X_{(Z)}$), to (*E*)-3-hexene ($X_{(E)}$), to *n*-hexane (X_n), the 3-hexyne total conversion (X_T) and the selectivity

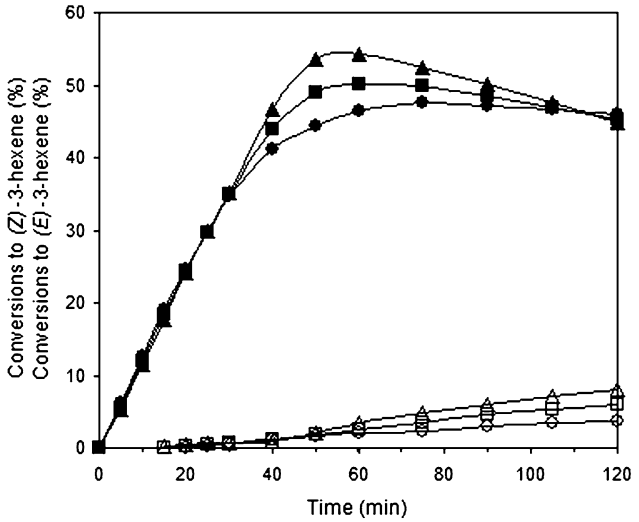

Fig. 3 Conversion to (*Z*)-3-hexene (%) (*filled symbols*) and to (*E*)-3-hexene (%) (*hollow symbols*) as a function of time for the Lindlar catalyst, measured at 150 kPa and different temperatures: $T_1 = 275$ K (●), $T_2 = 290$ K (■) and $T_3 = 303$ K (▲)

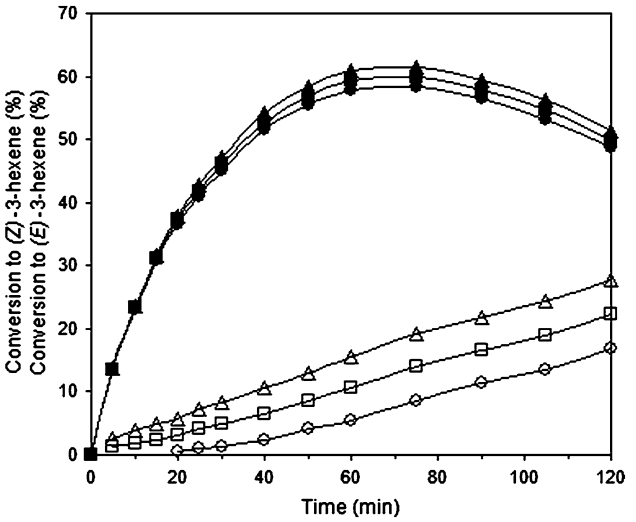

Fig. 5 Conversion to (*Z*)-3-hexene (%) (*filled symbols*) and to (*E*)-3-hexene (%) (*hollow symbols*) as a function of time for the pure $[PdCl_2(NH_2(CH_2)_{12}CH_3)_2]$ complex, measured at 150 kPa and different temperatures: $T_1 = 275$ K (●), $T_2 = 290$ K (■) and $T_3 = 303$ K (▲)

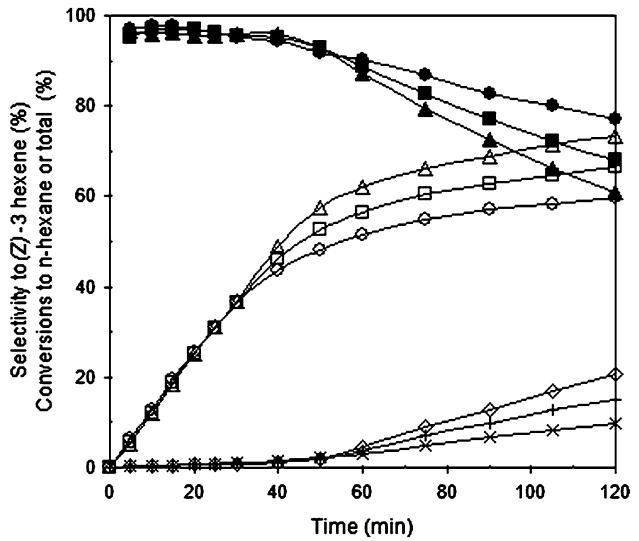

Fig. 4 Selectivity to (*Z*)-3-hexene (%) (*filled symbols*) and 3-hexyne total conversion (%) (*hollow symbols*) as a function of time for the Lindlar catalyst, measured at 150 kPa and different temperatures: $T_1 = 275$ K (●), $T_2 = 290$ K (■) and $T_3 = 303$ K (▲); and conversion to *n*-hexane (%) at $T_1 = 275$ K (*x*), $T_2 = 290$ K (+) and $T_3 = 303$ K (◇)

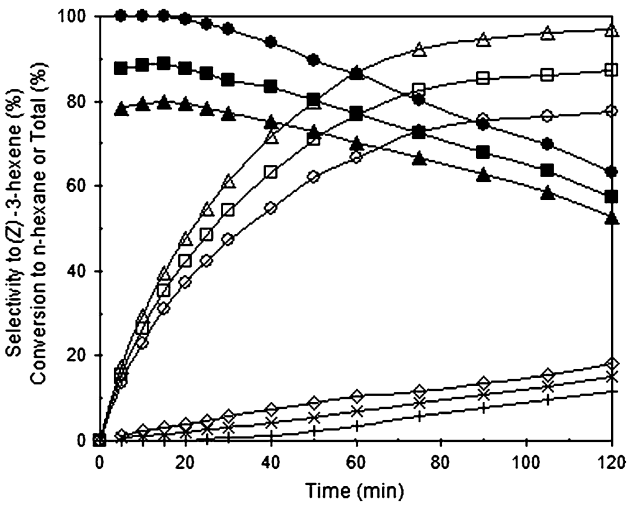

Fig. 6 Selectivity to (*Z*)-3-hexene (%) (*filled symbols*) and 3-hexyne total conversion (%) (*hollow symbols*) as a function of time for the pure $[PdCl_2(NH_2(CH_2)_{12}CH_3)_2]$ complex, measured at 150 kPa and different temperatures: $T_1 = 275$ K (●), $T_2 = 290$ K (■) and $T_3 = 303$ K (▲); and conversion to *n*-hexane (%) at $T_1 = 275$ K (*x*), $T_2 = 290$ K (+) and $T_3 = 303$ K (◇)

to (*Z*)-3-hexene ($S_{(Z)}$) are plotted as a function of the reaction time, at each reaction temperature (275, 290 and 303 K). Table 2 presents the conversion to (*Z*)-3-hexene and the 3-hexyne total conversion, and the selectivities to (*Z*)-3-hexene ($S_{(Z)}$), to (*E*)-3-hexene ($S_{(E)}$) and to *n*-hexane (S_n) obtained at each temperature for the three catalysts at 50 and 120 min operation time.

4 Discussion

4.1 Complex Characterization

The Pd:Cl:N molar ratios for the pure complex calculated from the weight percent values and the molar masses of these elements, can be expressed as ca. 1:2:2, respectively.

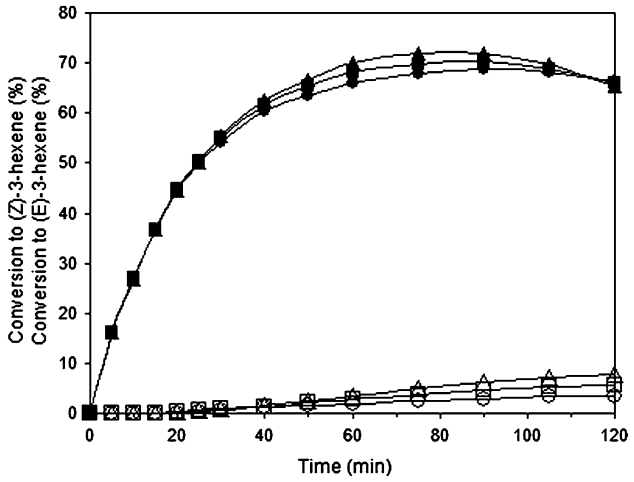

Fig. 7 Conversion to (*Z*)-3-hexene (%) (*filled symbols*) and to (*E*)-3-hexene (%) (*hollow symbols*) as a function of time for the alumina supported $[PdCl_2(NH_2(CH_2)_{12}CH_3)_2]$ catalyst, measured at 150 kPa and different temperatures: $T_1 = 275$ K (●), $T_2 = 290$ K (■) and $T_3 = 303$ K (▲)

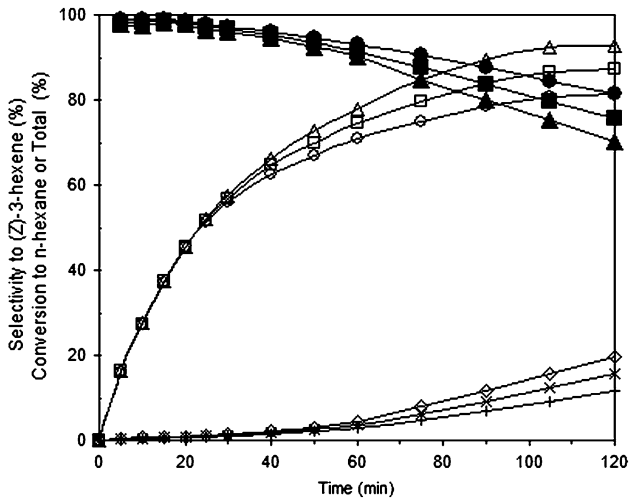

Fig. 8 Selectivity to (*Z*)-3-hexene (%) (*filled symbols*) and 3-hexyne total conversion (%) (*hollow symbols*) as a function of time for alumina supported $[PdCl_2(NH_2(CH_2)_{12}CH_3)_2]$ catalyst, measured at 150 kPa and different temperatures: $T_1 = 275$ K (●), $T_2 = 290$ K (■) and $T_3 = 303$ K (▲); and conversion to *n*-hexane (%) at $T_1 = 275$ K (*x*), $T_2 = 290$ K (+) and $T_3 = 303$ K (◇)

As presented in Table 1, the Pd $3d_{5/2}$, Cl $2p_{3/2}$ and N $1s_{1/2}$ peaks BE and superficial atomic ratios N/Pd and Cl/Pd of the pure and the fresh supported complex are almost the same. It can be observed that the atomic ratios N/Pd and Cl/Pd are around 2, in accordance with the centesimal composition determined via chemical analysis. These results indicate that the pure complex is not destroyed when it is anchored on the alumina. According to these facts the complex is tetra-coordinated, and even supported, it maintains its chemical identity. The BE for the pure complex are those characteristic of chlorine in a chloride species, to palladium with a +2 oxidation state, and to nitrogen corresponding to an ammonium-like nitrogen [35, 36]; this information suggests a bonding character for the N lone pair towards an electrophilic centre, in this case the palladium atom.

As indicated in the previous section, the Pd $3d_{5/2}$ peak BE for the Lindlar catalyst was 337.2 eV. The Pd $3d_{5/2}$ line for the Lindlar's catalyst is ca. 1 eV lower than that for the metal complex (supported or not), thus indicating that palladium presents different oxidation states on both the supported or unsupported complex and the Lindlar catalyst.

The FTIR spectra for the pure TDA and for the fresh unsupported palladium complex (Fig. 1a, b respectively) show frequencies corresponding to the characteristic peaks of a primary aliphatic amine, "that is: NH2 stretching around 3,100–3,600 cm^{-1} (A); CH stretching around 2,800–3,000 cm^{-1}; NH2 bending around 1,600–1,700 cm^{-1} (B); CH bending around 1,300–1,500 cm^{-1}, and CN stretching around 1,000–1,200 cm^{-1} (C), in total accordance with data in the literature [37]". Although the curves depicted in Fig. 1a, b are quite similar, the one corresponding to the complex presents some shifts towards lower energies. Special attention is focused on the wave numbers related to the nitrogen atom because they are sensitive to bond formation during the complex synthesis. This is so because the amine is attached to the palladium atom through the nitrogen lone pair. The zones identified by A, B and C, are those in which the nitrogen surrounding is compromised [38]. Comparing Fig. 1a, b it can be seen from the complex spectrum (Fig. 1b) that bands in A, B and C ranges are present at lower energies. Also, when a primary NH_2 is bonded, the stretching absorption peaks are considerably different in shape and intensity from the original NH_2 bands [37]. This is a fact that can also be observed in the same spectrum. All this information suggests that the TDA is a part of the coordination sphere.

The FTIR spectrum for the alumina supported complex, fresh and after catalytic tests (Fig. 1c, d) shows some of the most remarkable peaks mentioned above "(CH stretching, strong; CH bending, weak and B, strong)", suggesting that the complex is present after its heterogenization. At this point it is remarked the presence of γ-Al_2O_3 dominant structure which masks part of the spectra of all supported species; "this is due to the very low metal loading in the heterogeneous catalyst (0.3 wt%)". The spectra of the alumina supported complex after catalytic test at 303 K (curve d in Fig. 1), is quite alike to that obtained for sample c, thus indicating that the same species are present after the catalytic procedures.

The spectra obtained for the alumina supported complex after catalytic tests at 275 and 290 K (not shown in Fig. 1) are identical to that depicted in Fig. 1d. This allows confirming that there was no modification of the anchored complex under reaction conditions.

The IR spectra presented in Fig. 2a, b show the peaks corresponding to the Pd-ligand vibrations [39] for the pure and the adsorbed species. In both cases the complex can be considered the trans-isomer because of the presence of single peaks, which obey the principle of mutual exclusion, typical of centre-symmetric species, in this situation local D_2 h symmetry [40].

The results obtained from centesimal composition, IR and XPS techniques suggest that the complex empirical formula could be $[PdCl_2(NH_2(CH_2)_{12}CH_3)_2]$, and that the species maintains its identity after heterogenization and even after being catalytically evaluated.

4.2 Complex Leaching Evaluations

The activity of the anchored complex remained constant after 100 h length runs in toluene solution, and the Pd/Al atomic ratio was 0.088; this value is identical to the atomic ratio of the fresh supported complex.

On the other hand, no Pd was detected on all the remaining solutions for the heterogeneous catalytic tests by means of atomic absorption spectroscopy analysis [26].

The constancy of activity, the absence of Pd in the remaining solutions and the constancy of Pd/Al ratio, reveal that the complex is neither destroyed nor leached under the reaction conditions.

4.3 Catalytic Hydrogenation: Influence of the Reaction Temperature

The semi-hydrogenation of internal alkynes over Pd-containing catalysts typically results in the predominant formation (*Z*)-alkene stereo-isomers [3] accompanied by the production of alkanes (through over hydrogenation) and of (*E*)-alkenes, which may be formed either as initial products or via $Z \rightarrow E$ isomerization [11, 25].

For the Lindlar catalyst, at the three temperatures evaluated (275, 290 and 300 K), the initial products detected were only (*Z*)-3-hexene and *n*-hexane; (*E*)-3-hexene was detected after 20 min of hydrogenation at 275 K or after 15 min at 290 or 303 K. From Figs. 3 and 4 it is observed that up to 30 min of operation time, the production of (*Z*)-3-hexene, (*E*)-3-hexene and *n*-hexane were independent of the reaction temperature. From this time to the end of the run the product distribution was a function of the hydrogenation temperature, showing a maximum conversion to (*Z*)-3-hexene at 60 min (between 46 and 54%), as the temperature was raised up. In Fig. 3 it is noted that, at 290 or 303 K, after 60 min of the reaction course, the conversion to (*E*)-3-hexene increased slightly as the conversion to (*Z*)-3-hexene decreased slightly, suggesting an isomerization reaction [11, 25]. Only at 275 K after 60 min of reaction, the conversion to (*E*)-3-hexene increased very slightly, but the conversion to (*Z*)-3-hexene

Table 2 3-hexyne total conversion (X_T), conversions to (*Z*)-3-hexene ($X_{(Z)}$) and selectivities to (*Z*)-3-hexene, (*E*)-3-hexene and *n*-hexane ($S_{(Z)}$, $S_{(E)}$ and S_n, respectively) for the following catalysts: Lindlar, $[PdCl_2(TDA)_2]$ complex unsupported and anchored on γ-Al_2O_3

Reaction time (min)	Catalyst	*T* (K)	X_T (%)	$X_{(Z)}$ (%)	$S_{(Z)}$ (%)	$S_{(E)}$ (%)	S_n (%)
50	Lindlar	275	48	44	92	3	5
		290	53	49	93	3	4
		303	57	53	93	4	3
	Pd-TDA	275	62	56	90	7	4
		290	71	57	80	12	8
		303	80	58	73	16	11
	Pd-TDA/Al_2O_3	275	67	64	95	2	3
		290	70	66	94	3	3
		303	72	67	93	3	4
120	Lindlar	275	60	46	77	6	17
		290	66	45	68	9	23
		303	73	44	61	11	28
	Pd-TDA	275	77	48	63	22	15
		290	87	50	57	26	17
		303	97	51	53	28	19
	Pd-TDA/Al_2O_3	275	81	66	81	3	15
		290	87	65	75	6	18
		303	93	65	70	8	21

Reaction conditions: molar ratio 3-hexyne/Pd = 8400, hydrogen pressure 150 kPa, and different reaction temperatures (275, 290 and 303 K) at 50 or 120 min of reaction

remained practically constant. From 50 up to 120 min, the highest amount of (*E*)-3-hexene and *n*-hexane were obtained when the reaction temperature was 303 K (Figs. 3 and 4). According to Fig. 4 the Lindlar catalyst exhibited initially a rapid increase of the 3-hexyne total conversion with the course of reaction; after 25 min the higher 3-hexyne total conversions were obtained for the highest temperature. Also, in this figure, it is noted that up to 50 min of reaction time, the stereo-selectivity to (*Z*)-alkene formation was remarkably high (>90%) at the three temperatures evaluated; this implies that the amount of side-products obtained was negligible. Figure 4 also shows that the selectivity to (*Z*)-alkene decreased after 50 min of operation; this decrease in $S_{(Z)}$ is more evident as the temperature was raised up. Also it may be observed a marked drop in $S_{(Z)}$ at 303 K. In Table 2 are detailed the selectivities to (*E*)-3-hexene values detected at 120 min for the Lindlar catalyst: 6% (275 K), 9% (290 K) and 11% (303 K). As shown in Table 2, the selectivities to *n*-hexane formation via over-hydrogenation proved to be somewhat higher than $S_{(E)}$; at 120 min the S_n values are: 17% (275 K), 23% (290 K) and 28% (303 K).

For the unsupported complex at 290 and 303 K the initial products detected were (*Z*)-3-hexene, (*E*)-3-hexene and *n*-hexane. These evidences suggest that the (*E*)-alkene may be formed directly from the 3-hexyne hydrogenation and/or via a $Z \rightarrow E$ isomerization. On the other hand, the production of *n*-alkane took place through 3-hexyne over-hydrogenation [25]. Meanwhile at 275 K neither (*E*)-3-hexene nor *n*-hexane products were detected until 20 min of reaction; this suggests an isomerization mechanism to the production of (*E*)-alkene at the lowest reaction temperature evaluated. In Fig. 5 it can be observed that the unsupported complex showed comparable conversions to the (*Z*)-alkene at the different conditions throughout the reaction time, slightly higher at 303 K, showing the maximum ($X_{(Z)} \approx 60\%$) at $\sim$60 min. On the other hand, the conversion to (*E*)-3-hexene increased markedly with the reaction temperature; the profiles practically raised constantly from the beginning of the hydrogenation process. The conversion to *n*-hexane profiles (shown in Fig. 6) are very similar to those corresponding to the conversions to (*E*)-alkene (Fig. 5), but they are, at the three temperatures considered, slightly lower (see Figs. 5, 6; also compared in Table 2 for the unsupported catalyst selectivities to *n*-hexane and (*E*)-hexane at 50 or 120 min). From Fig. 6 it is observed that, as the reaction temperature was increased, the 3-hexyne total conversion increased markedly, but the (*Z*)-alkene stereo-selectivities decreased constantly. Only at a temperature of 275 K the stereo-selectivity to (*Z*)-alkene formation was high up to 50 min of reaction ($S_{(Z)} > 90\%$, from Fig. 6). At this reaction temperature only slight amounts of by-products were obtained for the unsupported catalyst, (*E*)-alkene and *n*-alkane were first detected at a 3-hexyne total conversion of 37% (at 20 min, Figs. 5, 6). In Table 2 it can be noted that, for the three temperatures, the maximum selectivities to (*E*)-hexene obtained at 120 min (22, 26 and 28% as the temperature was increased) are markedly higher than those obtained for the Lindlar catalyst at the same conditions (6, 9 and 11%, respectively). It can be observed from Fig. 6 that, for the unsupported catalyst, the higher 3-hexyne total conversions were obtained at 303 K but, at this temperature, the selectivity to (*Z*)-alkene was lower than 80%, indicating higher production of by-products: (*E*)-alkene and *n*-alkane. Also, for the unsupported Pd-TDA complex, it is noted from Figs. 5 and 6 that, as the temperature was raised, the yield of (*Z*)-alkene was slightly improved, but the production of the undesirable products, (*E*)-alkene and *n*-hexane, increased markedly. Up to 60 min, for the unsupported catalyst the conversion to (*Z*)-alkene values increased slightly as the temperature was raised, but the corresponding stereo-selectivity decreased notoriously.

For the Pd-TDA alumina supported catalyst, (*E*)-3-hexene was first detected at a 3-hexyne total conversion of 51% (25 min at 275 K) or 45% (20 min for 290 K or 303 K), suggesting that, at the three temperatures evaluated, (*E*)-3-hexene was produced by isomerization. At the same time, independently of the reaction temperature, *n*-hexane was detected from the beginning of the reaction, suggesting that *n*-alkane was produced by over-hydrogenation. From Figs. 7 and 8 it can be observed that for the Pd-TDA anchored complex, up to 60 min, the amount of side-products formed was negligible, with a stereo-selectivity to (*Z*)-3-hexene higher than 90% and a maximum conversion to (*Z*)-3-hexene ca. 68% (303 K). In Table 2 it is shown that the maximum values of stereo-selectivities to (*E*)-alkene were slightly lower than those obtained for the Lindlar catalyst: 3% (275 K), 6% (290 K) and 8% (303 K) at 120 min. The maximum selectivity to *n*-hexane values were obtained at 120 min and proved to be higher than the selectivity values to (*E*)-3-hexene; also they were similar to those obtained under identical conditions using the Lindlar catalyst: 15% (275 K), 18% (290 K) and 21% (303 K), as indicated in Table 2.

Comparing Figs. 4 and 8 it can be observed that throughout the reaction time, for each temperature, the anchored complex showed very similar (*Z*)-stereo selectivities, higher total alkyne conversions and consequently, higher (*Z*)-alkene conversions than those obtained with the Lindlar catalyst. Furthermore, these facts suggest that both the Lindlar and the Pd-TDA alumina supported catalysts should have similar reaction mechanisms and slightly different (*Z*)-3-hexene formation reaction rate.

Table 2 shows that at 50 min of operational time, as the reaction temperature was increased: (1) for the Lindlar

catalyst both the conversion to (*Z*)-3-hexene and the 3-hexyne total conversion increased, but the selectivity to (*Z*)- or to (*E*)-3-hexene and to *n*-hexane values remained almost constant; (2) for the unsupported Pd-TDA complex both the 3-hexyne total conversion and the side-products selectivities increased notoriously; consequently the selectivity to (*Z*)-alkene decreased abruptly, while the conversion to (*Z*)-3-hexene remained almost constant; (3) for Pd-TDA/γ-Al_2O_3 the 3-hexyne total conversion slightly increased with the reaction temperature, while the (*Z*)-alkene conversion and the selectivities to (*Z*)- or to (*E*)- alkenes and to *n*-hexane remained almost constant at the three temperatures studied. At 50 min reaction time, from Table 2 it can be concluded, on the one hand, that the unsupported complex has (*Z*)-alkene selectivities comparable to those of the Lindlar catalyst only at 275 K. Also, at this temperature and 50 min, the Pd-TDA complex presents a better yield to the desired product: the Lindlar catalyst conversion to (*Z*)-3-hexene was 44% and that of the unsupported complex was 56% (27% higher). On the other hand, at 50 min and under identical conditions, the supported complex presented selectivity to (*Z*)-3-hexene values comparable to those corresponding to the Lindlar catalyst (higher than 90%). Also, the Pd-TDA/γ-Al_2O_3 presented a conversion to (*Z*)-3-hexene higher than that obtained with the Lindlar catalyst, mainly al 295 K.

Moreover, in Table 2 at 120 min of reaction time, it is noted that when the reaction temperature is increased, the three catalysts had identical behavior: the total alkyne conversion increased gradually, and the selectivity to (*Z*)-3-hexene decreased markedly. It can be noted that at 120 min for the unsupported complex, the 3-hexyne total conversion was higher than that corresponding to the Lindlar catalyst, but the (*Z*)-alkene selectivities were lower. However, the conversion to (*Z*)-alkene values of the unsupported complex were slightly higher than the Lindlar ones (around 50 and 45%, respectively). At 120 min the Pd-TDA anchored complex run at the different temperatures, presented a 3-hexyne total conversion higher than that of the Lindlar catalyst (relative differences between 35% at 275 K and 27% at 303 K). Pd-TDA/γ-Al_2O_3 has also a selectivity to (*Z*)-3-hexene slightly higher than that of the Lindlar catalyst, and presented higher conversion to (*Z*)-3-hexene values.

Comparing the profiles of Figs. 3, 5 and 7 at each reaction temperature it may be concluded the following order of catalysts: (1) to optimize the formation of (*Z*)-3-hexene: Pd-TDA/γ-Al_2O_3 > Pd-TDA > Lindlar; (2) to optimize the formation of (*E*)-3-hexene: unsupported complex $\gg$ Lindlar $\approx$ alumina supported Pd-TDA complex.

From Figs. 3, 4, 5, 6, 7, 8 and Table 2, for $S_{(Z)}$ values not lower than 90% it can be clearly determined the best temperature and time values to obtain the highest conversion to (*Z*)-3-hexene for each system: (1) Lindlar catalyst, 303 K and 50 min; (2) unsupported complex, 275 K and 50 min; (3) supported complex, 303 K and 60 min. At these optimum reaction conditions, the non-supported palladium complex showed a selectivity to (*Z*)-3-hexene comparable to that of the Lindlar catalyst and had higher 3-hexyne total conversion and consequently higher conversion to (*Z*)-3-hexene than the Lindlar catalyst. On the other hand, the heterogeneous Pd-TDA complex evaluated at 60 min and 303 K showed a similar selectivity to (*Z*)-alkene compared to that obtained with the Lindlar catalyst and showed markedly higher 3-hexyne total conversion and conversion to (*Z*)-alkene. Consequently, these results suggest that the palladium(II) complex, supported or not, are active and stereo-selective catalysts for the semi-hydrogenation of the relatively high molecular weight internal alkyne 3-hexyne. However, the unsupported Pd-TDA catalyst has significant shortcomings because, after reaction, the complex should be recovered from the remaining solutions by careful and costly purification methods.

The supported complex is considerably more active and stereo-selective for the selective hydrogenation of 3-hexyne relative to the unsupported complex.

Molecular orbitals with symmetries corresponding to the irreducible representations of the molecular point group automatically satisfy the Fock equation. For complex species the terminal atom symmetry orbital (TASO)/molecular orbitals (MO) and the metal atomic orbitals are taken into account to explain metal-ligand bonding according to their symmetry properties. In this respect, the (n^{-1})d and ns metal atomic orbitals are those that match best the energy of the TASO/MO. Based on this, the anti-bonding MO have considerably more metal character than ligand character; anti-bonding MO lie high in energy. The most probable relative energy distribution of these anti-bonding MO for Pd(II) (d^8), predicted by means of the angular overlap model (AOM), is as follows in an increasing order of energy: non-bonding (dxz), double-degenerate $2e_\pi$ [(dxy, dyz)*], e_σ [(dz^2)*] and $3e_\sigma$ [$(dx^2 - y^2)$*] [32]. Assigning the eight electrons to this scheme, it turns out that dz^2 and $dx^2 - y^2$ are the HOMO and LUMO frontier orbitals, respectively. The HOMO orbital is useful to produce the cleavage of the H–H bonding while the LUMO orbital can receive electron density from the substrate molecule, what means to activate 3-hexyne for the semi-hydrogenation reaction. In addition, there could be some extra 3-hexyne molecules activated by their possible electron-donating interaction with the acidic Lewis sites of the support. This fact makes the reactant concentration around the supported complex catalyst higher than in the

bulk solution. Such an argument could explain the high activity and selectivity of this catalytic system.

5 Conclusions

The dichlorobis (tridecylamine) palladium(II) complex was prepared by using $PdCl_2$ and tridecylamine (TDA). The synthesized complex was purified and anchored on γ-Al_2O_3. Both complexes, pure and heterogenized, were characterized by centesimal composition, X-ray photoelectron spectroscopy and infrared spectroscopy (FTIR and IR). Chemical analysis results showed that Pd, Cl and N elements are present in the sample with a molar ratio equal to 1:2:2. XPS results indicated that the complex is tetra-coordinated and that, even supported, it maintains its chemical identity. IR results indicated that, for the pure and the anchored complex, the TDA molecule is part of the palladium coordination sphere, and in both cases the complex can be considered a trans isomer. These characterization techniques suggested that the complex empirical minimum formula could be $[PdCl_2(TDA)_2]$.

The unsupported and the supported palladium complex were used as catalysts for the semi-hydrogenation of 3-hexyne (an internal alkyne); Lindlar catalyst was used for comparative determinations. The influence of the temperature was studied for the three catalytic systems, at 275, 290 and 303 K. The hydrogen pressure was150 kPa and the molar ratio of alkyne to Pd was 8,400.

All of the catalysts, whatever the temperature, showed the semi-hydrogenation of 3-hexyne as the main reaction pathway, resulting in the predominant formation of (*Z*)-3-hexene. In all the cases, the maximum 3-hexyne total conversion was achieved at 303 K. Also it was found that, the highest selectivities to (*Z*)-species were observed from the beginning of the reaction up to 50 or 60 min (depending on the catalytic system). The selectivity to (*Z*)-alkene for the Lindlar catalyst and for the Pd-TDA anchored complex, up to 50 min of reaction time, were independent of the reaction temperature. Only for the unsupported complex the highest selectivities to (*Z*)-alkene was achieved at the lowest temperature (275 K).

For $S_{(Z)}$ values not lower than 90% the optimum time and temperature values found for each catalyst were: (I) 50 min of operational time and 303 K for the Lindlar catalyst; (II) 50 min and 275 K for the Pd-TDA unsupported complex; and (III) 60 min and 303 K for the alumina supported Pd-TDA complex Under these operational conditions, the production of (*Z*)-3-hexene with the three catalysts presented the following order: $[PdCl_2(TDA)_2]/\gamma$-Al_2O_3 > $[PdCl_2(TDA)_2]$ > Lindlar. This indicates that the Pd-TDA complex, supported or not, is an active and stereo selective system for the semi-hydrogenation of 3-hexyne. The results obtained indicate that the supported Pd-TDA complex is not destroyed under the reactions conditions and that there is no leaching of the complex during the catalytic evaluations. The anchored palladium complex shows higher activity and selectivity than the same complex unsupported; the different behavior between both palladium species can be attributed, at least partially, to electronic and geometrical effects.

Acknowledgments Financial support by UNL, CONICET and ANPCyT, and the donation of FTIR and XPS equipment by JICA, are acknowledged. The authors also acknowledge José Paredes for technical support.

References

1. Chen B, Dingerdissen U, Krauter JGE, Lansink Rotgerink HGJ, Möbus K, Ostgard DJ, Panste P, Riermeir TH, Seebald S, Tacke T, Trauthwein H (2005) Appl Catal A Gen 280:17–46
2. Mastalir Á, Király Z (2003) J Catal 220:372–381
3. Molnár Á, Sárkány A, Varga M (2001) J Mol Catal A: Chem 173:185–221
4. Lindlar HH, Dubuis R, Jones FN, McKusick BC (1966) Org Synth 46:89 Coll. 5 (1973) 880
5. Choudary BM, Lakshmi Kantam M, Mahender Reddy N, Koteswara Rao K, Haritha Y, Bhaskar V, Figueras F, Tuel A (1999) App Catal A Gen 181:139–144
6. Mastalir Á, Király Z, Berger F (2004) Appl Catal A: Gen 269: 161–168
7. Mastalir Á, Rác B, Király Z, Molnár Á (2007) J Mol Catal A: Chem 264:170–178
8. Mastalir A, Rác B, Király Z, Tasi G, Molnár Á (2007) Catal Comm in press
9. Gruttadauria M, Noto R, Deganello G, Liotta LF (1999) Tetrahedron Lett 40:2857–2858
10. Lennon DD, Marshall R, Webb. G, Jackson SD (2000) Stud Surf Sci Catal 130:245–250
11. Marín-Astorga N, Pecchi G, Fierro JLG, Reyes P (2003) Catal Lett 91(1–2):115–121
12. Mastalir Á, Király Z, Szöllósi Gy, Bartók M (2000) J Catal 194:146–152
13. Yu J, Spencer JB (1998) Chem Comm. 1103–1104
14. Nijhuis TA, van Koten G, Kapteijn F, Moulijn JA (2003) Catal Today 79–80:315–321
15. Brown ChA, Ahuja VK (1973) J Org Chem 38(12):2226–2230
16. Choi J, Yoon NM (1996) Tetrahedron Lett 37(7):1057–1060
17. Guczi L, Schay Z, Stefler Gy, Liotta LF, Deganello G, Venezia AM (1999) J Catal 182:456–462
18. Coq B, Figueras F (2001) J Mol Catal A: Chem 173(1–2):117–134
19. Nijhuis TA, van Koten G, Moulijn JA (2003) Appl Catal A: Gen 238:259–271
20. Giannandrea R, Mastrorilli P, Zaccaria G, Nobile CF, Molec J (1996) Catal A: Chem 109:113–117
21. Kameda N, Yoneda T (1999) J Chem. Soc. of Japan, Chemistry and Industrial Chemistry, No 1:33
22. Lough AJ, Morris RH, Ricciuto L, Schleis T (1998) Inorg Chim Acta 270:238–246
23. Quiroga M, Liprandi D, L'Argentière P, Cagnola E (2005) J Chem Technol Biotechnol 80:158–163

24. de Wolf E, Spek AL, Kuipers BWM, Philipse AP, Meeldijk JD, Bomans PHH, Frederik PM, Deelman BJ, van Koten G (2002) Tetrahedron 58:3911–3922
25. Papp A, Molnár A, Mastalir Á (2005) Appl Catal A: Gen 289:256–266
26. L'Argentière PC, Cagnola EA, Quiroga ME, Liprandi DA (2002) Appl Catal A: Gen 226:253–263
27. L'Argentière PC, Quiroga ME, Liprandi DA, Cagnola EA, Román-Martínez MC, Díaz-Auñon JA, Salinas-Martínez de Lecea C (2003) Catal Lett 87(3–4)
28. Díaz-Auñon JA, Román-Martínez MC, Salina-Martínez de Lecea C, L'Argentière PC, Cagnola EA, Liprandi DA, Quiroga ME (2000) J Mol Catal A: Chem 256:243
29. Seoane XL, L'Argentière PC, Fígoli NS, Arcoya A (1992) Catal Lett 16:137
30. Holland FA, Chapman FS (1976) Liquid mixing and processing in stirred tanks, vol 2. Reinbold, New York
31. Le Page JF (1978) Catalyse de contact. Editions Technip, Paris
32. Quiroga M, Liprandi D, Cagnola E, L'Argentière P (2007) Appl Catal A: Gen 326:121–129
33. Mallat T, Petro J, Szabó S, Sztatisz J (1985) React Kinet Catal Lett 29:353–361
34. Liprandi D, Quiroga M, Cagnola E, L'Argentière P (2002) Ind Eng Chem Res 41:4906–4910
35. Wagner CD, Riggs WM, Davis LE, Moulder JF (1978) Handbook of X-ray photoelectron spectroscopy. In: Mullenberg GE (ed.) Perkin-Elmer Corporation, Eden Preirie
36. NIST X-ray Photoelectron Spectroscopy Database NIST Standard Reference Database 20, Version 3.4 (Web Version), National Institute of Standards and Technology, USA, 2003
37. Pouchert CJ (1981) The Aldrich library of infrared spectra, 3rd edn. Aldrich Chemical Company Inc, Wisconsin, pp 163–164
38. Silverstein RM, Clayton-Basler G, Morril TC (1991) Spectrometric identification of organic compounds, 5th edn. Wiley, New York, pp 123–124
39. Durig JD, Mitchell BR (1967) Appl Spectrosc 21:222
40. L'Argentière PC, Liprandi DA, Cagnola EA, Fígoli NS (1997) Catal Lett 44:101–107